

Water Resources Research

RESEARCH ARTICLE

10.1002/2017WR020843

Key Points:

- Climatic and physiographic variables explained 81% of the characteristics that control precipitation partitioning across watersheds examined
- The Budyko relationship using model derived watershed characteristics resemble results from sophisticated land-surface hydrologic models
- Projected changes in water balance using the Budyko relationship show declines in runoff for most of the United States

Supporting Information:

- Supporting Information S1
- Data Set S1

Correspondence to:

J. T. Abatzoglou,
jabatzoglou@uidaho.edu

Citation:

Abatzoglou, J. T., and D. L. Ficklin (2017), Climatic and physiographic controls of spatial variability in surface water balance over the contiguous United States using the Budyko relationship, *Water Resour. Res.*, 53, 7630–7643, doi:10.1002/2017WR020843.

Received 3 APR 2017

Accepted 6 AUG 2017

Accepted article online 14 AUG 2017

Published online 1 SEP 2017

Climatic and physiographic controls of spatial variability in surface water balance over the contiguous United States using the Budyko relationship

John T. Abatzoglou¹  and Darren L. Ficklin² 

¹Department of Geography, University of Idaho, Moscow, Idaho, USA, ²Department of Geography, Indiana University, Bloomington, Indiana, USA

Abstract The geographic variability in the partitioning of precipitation into surface runoff (Q) and evapotranspiration (ET) is fundamental to understanding regional water availability. The Budyko equation suggests this partitioning is strictly a function of aridity, yet observed deviations from this relationship for individual watersheds impede using the framework to model surface water balance in ungauged catchments and under future climate and land use scenarios. A set of climatic, physiographic, and vegetation metrics were used to model the spatial variability in the partitioning of precipitation for 211 watersheds across the contiguous United States (CONUS) within Budyko's framework through the free parameter ω . A generalized additive model found that four widely available variables, precipitation seasonality, the ratio of soil water holding capacity to precipitation, topographic slope, and the fraction of precipitation falling as snow, explained 81.2% of the variability in ω . The ω model applied to the Budyko equation explained 97% of the spatial variability in long-term Q for an independent set of watersheds. The ω model was also applied to estimate the long-term water balance across the CONUS for both contemporary and mid-21st century conditions. The modeled partitioning of observed precipitation to Q and ET compared favorably across the CONUS with estimates from more sophisticated land-surface modeling efforts. For mid-21st century conditions, the model simulated an increase in the fraction of precipitation used by ET across the CONUS with declines in Q for much of the eastern CONUS and mountainous watersheds across the western United States.

1. Introduction

Quantifying water availability, both in the present and in the future, is extremely important for both societal demands and ecosystem needs [Vörösmarty *et al.* 2000]. In regions where high-quality long-term hydrologic observations are sparse, water resources such as runoff is often quantified using hydrologic models. These models, however, are subject to uncertainties in hydrological model structure, simplification, and parameterization [Wilby and Harris 2006; Renard *et al.* 2010], particularly when applied to watersheds without observed data for calibration [Sivapalan *et al.* 2003]. Further, these models can be computationally expensive, often requiring high-performance computing when running models over continental scales, and may limit a comprehensive assessment of uncertainty in forcing data or climate change scenarios [Bossard *et al.* 2013; Elsner *et al.* 2014]. Hence, simplified water balance models that require a limited number of input variables remain popular in the literature for landscape scale estimates of surface hydroclimate [Schaake *et al.* 1996; McCabe and Wolock 2011; Abatzoglou *et al.* 2014].

Over longer time periods (e.g., multidecadal), the partitioning of precipitation (P) into evapotranspiration (ET) and surface runoff (Q) is pertinent to understanding the geographic variability of water resources. However, it is extremely difficult to estimate ET, particularly across regions of heterogeneous vegetation, soil, climate, and topography [Long *et al.*, 2014], and instead ET is often estimated for longer time steps (i.e., annual) as the residual of P minus Q for a given catchment when Q and P are accurately measured and intercatchment groundwater fluxes are negligible. At subcatchment scales or in ungauged watersheds, the partitioning of P is more challenging to estimate. To alleviate this difficulty, Budyko [1974] empirically showed a relationship between the partitioning of P and the ratio of potential evapotranspiration (PET) to P,

also known as the aridity index (PET:P). The Budyko curve, as it is often known by, is a nonlinear relationship constrained by the physical limits of atmospheric water demand (PET > ET) and supply (P > ET) that provides a means for partitioning of P into ET and Q for a given aridity index. The simplicity of the Budyko framework makes it attractive for examining spatial variability in the long-term average terrestrial water balance [Milly 1994; Potter et al. 2005], interannual variability [Yang et al. 2007], and response under changing climatic conditions [Liang et al. 2015]. Many studies have used the Budyko framework to quantify and separate the impacts of climate change and human activities on surface water runoff [Gardner, 2009; McMahon et al., 2011; Roderick and Farquhar, 2011; Zhan et al., 2013; Xu et al., 2014; Jiang et al., 2015].

Numerous studies have illustrated deviations from Budyko's original deterministic curve for individual catchments suggesting that other factors control the partitioning of P into ET and Q [Budyko, 1974; Milly, 1994; Donohue et al., 2012; Gentine et al., 2012; Li et al., 2013]. These variations can be numerically represented by the free parameter ω in the equation developed by Fu [1981], which is expressed as:

$$\frac{ET}{P} = 1 + \frac{PET}{P} - \left(1 + \left(\frac{PET}{P} \right)^\omega \right)^{\frac{1}{\omega}} \quad (1)$$

where ET is actual evapotranspiration, PET is potential evapotranspiration, P is precipitation. Equation (1) states the partitioning of P into ET and Q is a function of the aridity index and ω , with higher values of ω leading to higher ET:P ratios. The free parameter ω can be calibrated using historical Q and P for individual catchments, but lacks a physical meaning. Whereas the default value for ω is 2.6, ω exhibits substantial variability across catchments [e.g., Li et al. 2013] suggesting the need to better characterize the factors that contribute to its variability to improve upon continental-scale surface water balance estimates using the Budyko relationship.

Previous studies have explored both the spatial variability in ω and its relationship to environmental factors. Variations in ω have been found to be related to physical characteristics of the landscape, including climate, vegetation, soils, and topography. Climatic characteristics such as the seasonal synchronicity between P and PET [Milly, 1994; Wolock and McCabe, 1999; Potter et al., 2005; Gentine et al., 2012] and the proportion of precipitation falling as snow [Berghuijs et al., 2014] have been shown to alter ω . For example, greater synchronicity between P and PET (e.g., warm season dominant precipitation) generally enhances the fraction of P lost to ET and hence ω . Several studies have shown that vegetation type, cover, and productivity influence ω [Donohue et al., 2006; Li et al., 2013; Zhang et al., 2016], with higher values of ω in forested versus grassland catchments due to greater ET in forested catchments [Zhang et al., 2004]. Soil properties such as water holding capacity have been shown to influence ω as deeper soils allow for increased plant water use at the expense of Q [Milly, 1994; Wolock and McCabe, 1994; Zhang et al., 2001; Sankarasubramanian and Vogel, 2002; Porporato et al., 2004; Donohue et al., 2012]. Catchment slope can also influence the amount and timing of Q, which subsequently affects ET [Yang et al., 2007; Shao et al., 2012; Zhou et al., 2015]. While the effect of the individual environmental properties on ω have been explored, models have rarely attempted to evaluate how climatic, vegetation, topographic, and soil predictor variables collectively influence spatial variability in ω across broad scales [Sankarasubramanian and Vogel, 2002; Rodríguez-Iturbe et al., 2006; Shao et al., 2012; Zhou et al., 2015; Wang et al., 2016].

This paper evaluates the variability of ω and its associated drivers across the contiguous United States (CONUS) to develop an empirical model of ω . The motivation for advancing the empirical modeling of ω is to be able to use the model in the context of the Budyko equation described by Fu [1981] for estimating runoff across broad geographic regions [Li et al., 2013] and under future climatic conditions [Roderick and Farquhar, 2011]. Additionally, the Budyko relationship lends itself to an alternative approach for assessing the potential response of catchment water balance to climate change to complement other approaches [Vano and Lettenmaier, 2014].

2. Materials and Methods

2.1. Study Area and Streamflow Data

Streamflow discharge from United States Geological Survey Hydro-Climatic Data Network streamflow gauges (HCDN) [Slack and Landwehr, 1992] throughout the CONUS were acquired for 1980–2010. HCDN

gauges were selected given the relatively nominal human influence within the watersheds making them more suitable for assessing hydroclimatic relationships. Small watersheds ($<480 \text{ km}^2$) and watersheds with any incomplete years (more than 5 days of missing streamflow) from 1980 to 2010 were eliminated from subsequent analysis, leaving a total of 218 watersheds. We removed smaller watersheds due to potential inaccuracies in estimating catchment-averaged environmental variables from raster-based climate data at a 2.5 arc-minute ($\sim 16 \text{ km}^2$) since the ratio of the area of climate data pixels fully contained within the watershed to the area of watershed can be well below 1 for smaller watersheds. We also acquired streamflow discharge from gauges in the Model Parameter Estimation Experiment data set (MOPEX) [Duan *et al.*, 2006] for evaluating the model of ω developed with HCDN gauges. A total of 164 independent MOPEX watersheds that had complete streamflow data from 1980 to 2010 were used.

We calibrated ω for each watershed using equation (1) and mean annual P and PET (described below) for 1980–2010. The Budyko relationship assumes steady state conditions, nominal storage, and that moisture is not added or removed to the watershed via groundwater interaction or extracted from the watershed other than by ET [Roderick and Farquhar, 2011; Gentile *et al.*, 2012]. This calibration sought to minimize the mean absolute difference of observed Q and estimated Q (derived from equation (1)) using a uniform distribution of ω from 1.25 to 9 with 0.01 increments. Estimated values of ω were capped at 1.25 as this value reflects the minimum value for bare soil [Donohue *et al.*, 2012]. We excluded seven HCDN watersheds from subsequent analysis on the basis of implausible water balance characteristics including where $Q > P$ and where catchment-averaged $ET (P - Q) > PET$ [Peel *et al.*, 2010], as well as where the calibrated ω equaled 1.25. Hence, a total of 211 HCDN watersheds were used hereafter.

2.2. Environmental Predictors of ω

A set of geospatial climate, vegetation, soils, and topographic variables were used as explanatory predictors of spatial variability in ω based on prior studies (Table 1).

2.2.1. Climate

Climate data including daily maximum air temperature, minimum air temperature, precipitation, downward solar radiation, wind speed, and specific humidity for the years 1980–2010 were extracted from the gridded surface meteorological data set (gridMET) of Abatzoglou [2013]. gridMET is a hybrid of Parameter-elevation Regressions on Independent Slopes (PRISM) [Daly *et al.*, 2008] and the North American Land Data Assimilation System – Phase 2 (NLDAS-2) [Mitchell *et al.*, 2004] that yields daily data at a $\sim 4 \text{ km}$ spatial resolution. We estimate PET using Daily reference evapotranspiration (ETo) calculated using the Penman-Monteith method following Allen *et al.* [1998]. Note that ETo represents the reference evapotranspiration for a short well-watered grass with a static albedo of 0.23. Monthly climate normals for P, ETo, and mean temperature for the 1980–2010 period were used hereafter.

We used several climate measures as environmental predictors of ω . Monthly ETo and P were used to calculate Cumulative Moisture Surplus (CMS) [Wolock and McCabe, 1999] as:

$$\text{CMS} = \sum_{i=1}^{12} \frac{(P_i - ETo_i)}{\text{Dec.}} \quad \text{for } P_i > ETo_i \quad (2)$$

for each month (i). CMS was further expressed as the relative CMS (rCMS) by dividing it by annual P, and is a measure of seasonal asynchronicity between P and ETo. We also explored predictors of mean annual ETo,

Table 1. Pearson's Correlation Coefficients for Predictor Variables and Estimated Omega for 211 HCDN Watersheds^a

Variable	Description	Correlation (r)
ETo	Annual mean reference evapotranspiration	0.48
P	Annual mean precipitation	-0.52
AI (ETo/P)	Aridity index	0.67
rCMS	Cumulative moisture surplus divided by annual precipitation	-0.67
SF	Fraction of annual precipitation falling as snow	-0.50
AWC	Available water holding capacity in top 1.5 m of the soil	0.37
AWC:P	Ratio of AWC to mean annual precipitation	0.67
Mean slope	Watershed slope mean	-0.57
Standard deviation slope	Watershed slope standard deviation	-0.57
NDVI	Annual mean normalized difference vegetation index	-0.52
NPP	Annual mean net primary productivity	-0.35

^aAll correlations were significant at $p < 0.05$.

mean annual P, and the fraction of annual P falling as snow (SF) using the empirical precipitation phase typing approach of *Dai* [2008] using monthly mean temperature and precipitation.

In addition to developing and evaluating a model for ω for contemporary climate, we additionally use this model and the Budyko equation described by *Fu* [1981] to assess projected changes in land surface hydrology given downscaled mid-21st century climate model projections. Statistically downscaled climate projections from the Multivariate Adaptive Constructed Analogs (MACA) approach [*Abatzoglou and Brown*, 2012] that were developed using the gridMET forcing data were used for compatibility with the observational data set used in modeling ω . This exercise considered only the simple multimodel mean projection for monthly P, ETo, and mean temperature for the mid-21st century (2040–2069) taken from 20 climate models using the Representative Concentration Pathway 8.5 forcing experiment (supporting information Table S1). Nominal differences between observed (1980–2010) and downscaled multimodel mean late 20th century (1971–2000) climate from historical forcing experiments allow for a straightforward comparison between mid-21st century mean climate and the observed period. We calculated ETo using the Penman-Monteith method following *Allen et al.* [1998] using projected changes in the requisite statistically downscaled inputs of downward shortwave flux, vapor pressure, wind speed, and maximum and minimum temperature. Although increases in carbon dioxide concentrations have been argued to enhance water use efficiency and buffer increases in ETo that arise due to enhanced atmospheric vapor pressure deficit [*Donohue et al.*, 2010; *Swann et al.*, 2016], we do not account for this in our simple application.

2.2.2. Vegetation Indices

We considered two vegetation indices from remotely sensed imagery taken from Moderate Resolution Imaging Spectroradiometer (MODIS) satellite data averaged over the period 2002–2010 at a 1 km spatial resolution. Vegetation productivity was assessed using mean annual Net Primary Productivity (NPP) from MODIS [*Running et al.*, 2004]. NPP data for areas of urbanized landscapes, wetlands, perennial snow cover, sparsely vegetated lands, and freshwater bodies were considered missing. Second, we used annual mean Normalized Difference Vegetation Index (NDVI) as it has been shown to be an important explanatory variable for predicting variability in ω across very large watersheds globally [*Li et al.*, 2013]. A comprehensive assessment of the consortium of remotely derived data sets as they relate to the Budyko relationship is beyond the scope of this analysis.

2.2.3. Soils and Topography

Data on soil water holding capacity were acquired from State Soil Geographic (STATSGO) data set at a ~1 km resolution. We considered available water holding capacity (AWC) in the top 1.5 m of the soil column as a proxy for plant available water content. In addition, we considered the ratio of AWC to mean annual precipitation (AWC:P) following *Milly* [1994] and *Donohue et al.* [2012]. Slopes for the United States were extracted from the National Gap Analysis Program geospatial portal at a 30 m resolution. Slopes were estimated as a percent change of elevation for each 30 m grid cell.

2.3. Modeling ω

We conducted statistical analyses to relate calibrated ω to environmental predictors listed in Table 1. Predictors were spatially aggregated (using either the mean or standard deviation) over each HCDN or MOPEX watershed from data at their native resolution. First, Pearson's correlation coefficients were calculated between ω and each of the predictor variables to gauge simple linear relationships. Second, we developed a bivariate generalized additive model (GAM) of ω using each predictor variable independently to examine potential nonlinearities in the relationship between ω and each environmental variable. Previous studies have examined relationships and developed models using both linear [*Yang et al.*, 2007; *Xu et al.*, 2013] and nonlinear [*Shao et al.*, 2012] empirical approaches. We considered a nonlinear model given the potential nonlinear relationships between watershed characteristics and the *Fu*'s model parameter in the Budyko curve [e.g., *Wang et al.*, 2016]. Whereas GAMs have been used extensively in empirical ecological models [e.g., *Krawchuk et al.*, 2009; *Pausas and Ribeiro*, 2013], their use in hydrologic applications has been somewhat limited [e.g., *Chebana et al.* 2014]. GAMs are an extension of linear models but allow for the use of nonparametric smoothed functions as a response curve for each variable thus not requiring a predetermined form of the functional relationship between response variable and predictor. GAMs were fitted using the "mgcv" package from the R language using the Gaussian identity link that uses a thin plate splines basis [*R Core Team*, 2017; *Wood and Wood*, 2017]. GAMs provide easily interpretable results as they do not explicitly include interaction terms across response variables and the model the summation of values from

individual response curves using a link function. We do not assume that GAM are the optimal tool for empirical data analysis and modeling in the context of Budyko relationships, but instead may be a complementary approach to the existing set of regression approaches that have been explored [e.g., Yang *et al.*, 2007; Li *et al.*, 2013; Xu *et al.*, 2013].

Third, we developed a multivariate GAM using predictor variables that were complementary to one another. The GAM was built using stepwise forward regression that only considered significant ($p < 0.05$) terms added to the model. We did not consider the environmental variables of P, ETo, and the aridity index as part of the GAM given their intrinsic use in the Budyko equation. To minimize multiple collinearity and potential overfitting, we excluded variables from entering the stepwise regression model that exhibited strong correlation ($|r| > 0.6$) with terms already included.

We applied the GAM to estimate ω for MOPEX watersheds for validation purposes, and over the CONUS using predictors aggregated to the ~4 km spatial resolution of gridMET data. As a conservative approach for modeling ω across a broad geographic extent, we constrained variables to the range of values within the training HCDN data. This clamping (i.e., setting values outside the range of the training data to the maximum or minimum value) has the effect of avoiding uncertainties of extrapolating beyond the range of the historical data, but may also constrain the ability to predict ω in novel regions.

3. Results and Discussion

3.1. Spatial Patterns of Calibrated ω

The mean calibrated ω for HCDN and MOPEX watersheds (Figure 1) was 2.45 and 2.18, respectively, less than the default value of 2.6. However, there was substantial geographic variability in ω , which was also documented by Xu *et al.* [2013]. The standard deviation of ω was 0.7 and 0.46 for HCDN and MOPEX watersheds, respectively. Low ω values (<2) were found for the Pacific Northwest and northeastern United States, whereas the largest ω values (>3) were mainly found for watersheds across the Great Plains resembling patterns seen by Greve *et al.* [2015] and Zhou *et al.* [2015].

A couple of critical differences between calibrated ω in this study from previous studies are however apparent. First, unlike [Greve *et al.*, 2015] who showed $\omega > 3$ for many watersheds across the southeastern United States, our calibrated ω across the southeastern United States were generally between 2 and 3. Differences may also be a consequence of the approaches used in estimating PET, as well as different estimates of P. We estimated daily ETo following the Penman-Monteith approach for a reference grass surface, whereas Greve *et al.* [2015] used spatial estimates of pan evapotranspiration and Zhou *et al.* [2015] used coarser-resolution estimates of PET based on the Hamon method. Likewise, our ETo calculations followed the standardized ACSE approach and does not adjust for albedo during periods where snow cover may be present. This approach was used for transparency and reproducibility; however, it may result in positive ETo biases in some watersheds. The discrepancies in these studies highlights that ω estimates can be sensitive to the climatic inputs (P and PET), which could be the topic of future studies.

3.2. Bivariate Relationships to ω

Statistically significant ($p < 0.05$) relationships between ω and each of the predictors were found for HCDN watersheds using simple linear Pearson's correlation coefficients (Table 1). Positive correlations were found between ω and soil water holding capacity (AWC) as enhanced soil moisture storage increases infiltration, plant water availability, and ET for a given amount of P at the expense of Q [Zhang *et al.*, 2001]. Similarly, the AWC:P ratio exhibited a strong positive correlation (0.67) with ω . This is consistent with reduced Q potential (for a given P) in watersheds with deeper soils and low annual P [Milly, 1994]. The negative correlation between SF and ω is consistent with enhanced water yields in watersheds with higher SF [Berghuijs *et al.*, 2014]. Relative CMS exhibited a strong negative correlation with ω consistent with the influence of seasonal P-ETo asynchrony on water yields [Milly, 1994; Wolock and McCabe, 1999]. Both mean slope and the standard deviation of slope exhibited negative correlations with ω , consistent with the notion of Q being more easily generated in regions of complex terrain. Negative correlations were found between ω and both NPP and NDVI. These correlations suggest enhanced Q:P partitioning for a given aridity index for greater vegetation vigor or greenness, which is counter to the results found by Li *et al.* [2013] who showed strong positive correlations for very large ($>300,000 \text{ km}^2$) watersheds globally.

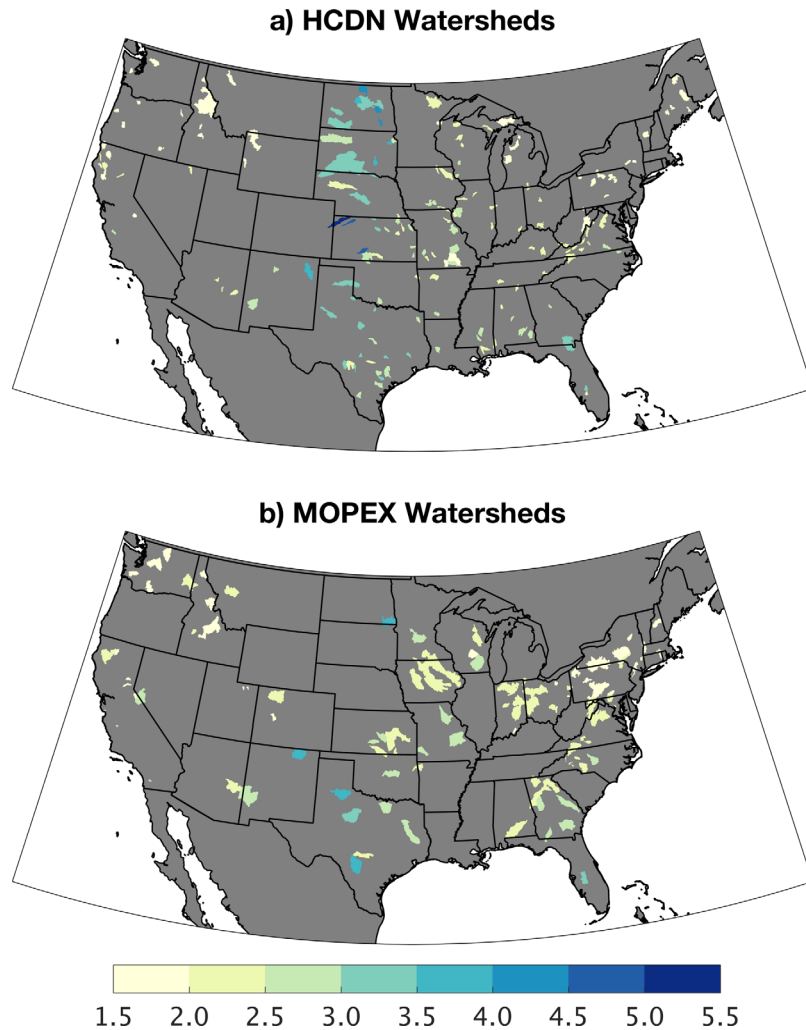


Figure 1. Calibrated ω for the 1980–2010 period for (a) HCDN watersheds and (b) MOPEX watersheds.

Bivariate GAM results generally showed directionally consistent relationships to those realized through simple linear relationships (Figure 2). For example, ω increases with ETo which is physically consistent with reduced Q potential. Substantial nonlinearities in the empirical relationships, however, were apparent for several variables. Watersheds with low rCMS (<0.15) had elevated ω consistent with a large portion of P being either seasonally synchronized with ETo, or where typically monthly ETo $>$ P. By contrast, ω values were lower for watersheds that exhibited greater P-ETo asynchrony, with ω plateauing for rCMS $>$ 0.4. Values of ω decreased rapidly with rising SF for watersheds that received between 15 and 25% of their annual precipitation as snow, with little additional influence for watersheds with substantially less or more SF. Finally, ω relationships with NDVI and NPP were unimodal and bimodal, respectively, with both showing higher ω in watersheds with relatively low vegetation vigor. It is worth noting that significant covariability across predictor variables may confound bivariate relationships shown here.

3.3. Modeled ω

The multivariate GAM final model explained 81.2% of the spatial variability in ω for HCDN watersheds and incorporated four terms: the ratio of AWC to annual P, relative CMS, mean watershed slope, and the fraction of precipitation falling as snow. All variables generally exhibited similar functional relationships in the multivariate GAM as in bivariate relationships (Figure 3). Per the construct of the GAM for ω , the influence of the modeled fit for each of the four predictor variables is additive to the overall intercept of the equation (supporting information Text S1). The GAM showed declines in ω with increased rCMS, and increases in ω where

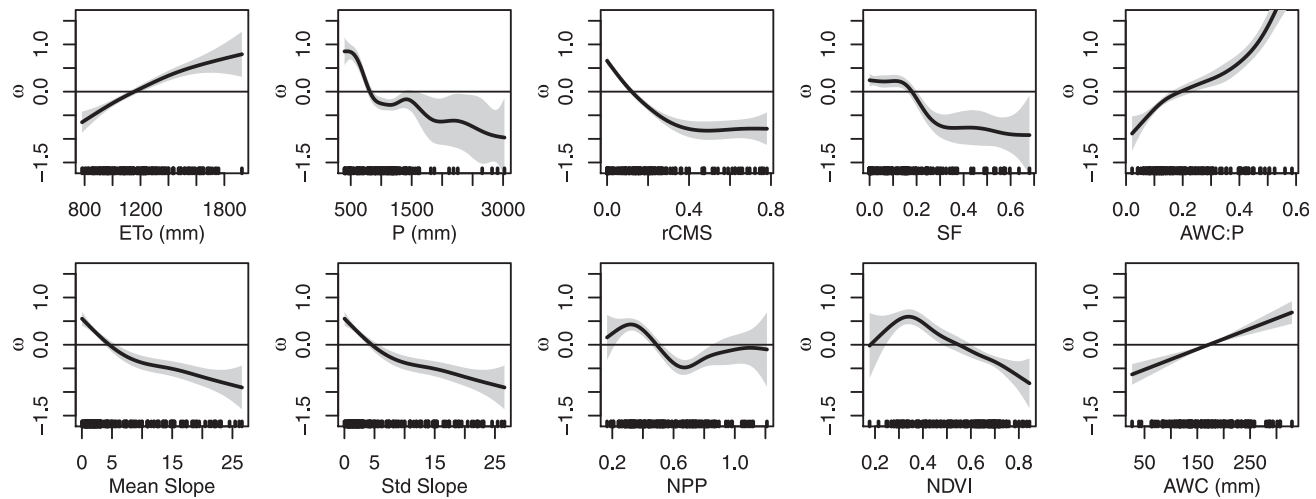


Figure 2. Bivariate response ω curves from the generalized additive model for HCDN watersheds with (top row, left to right) reference evapotranspiration (ETo), precipitation (P), relative cumulative moisture surplus (rCMS), fraction of annual precipitation falling as snow (SF), the ratio of available soil water holding capacity (AWC) to annual precipitation, (bottom row, left to right), mean watershed slope, standard deviation of watershed slope, net primary productivity (NPP), normalized different vegetation index (NDVI), and AWC. The grey shading in each plot depicts the 95% confidence interval of the relationship, with the black stripes along the x axis denoting the distribution of data from individual watersheds.

AWC:P > 0.4. The influence of mean slope in the multivariate GAM was nominal except in very flat terrain where it contributed to increased ω . SF had a subtle influence in the multivariate GAM, likely because of compensatory effects from other variables included in the GAM as watersheds with high values of SF, namely across mountain watersheds in the western United States, also generally had high rCMS and mean slope (supporting information Figure S1). Conceptually, the GAM suggests higher ω in watersheds with high AWC:P ratios, summer-dominant precipitation, shallow slopes, and small proportion of annual P as snow. Conversely, lower values of ω such as that seen across the mountainous western United States is consistent with the seasonal P-ETo mismatch, lower AWC:P ratios, steeper topography, and moderate SF ratios.

While vegetation cover and productivity exhibited strong relationships with ω in prior studies [Li *et al.*, 2013; Xu *et al.*, 2013], neither NPP nor NDVI provided additional explanatory power in the GAM (Figure 2). It is unclear whether these results are a consequence of the uncertainty in how vegetation dynamics fit into the Budyko framework [Zhang *et al.*, 2001; Oudin *et al.* 2008], the vegetation metrics we selected, or the fact that the climatic variables and AWC used in the GAM partially explain vegetation patterns [e.g., Stephenson, 1990], and in turn, the influence of vegetation of ω . We note that the vegetation metrics used here fail to adequately discriminate across vegetation types (e.g., deciduous versus evergreen) and their water use requirements, and that annual P was strongly positively correlated to both vegetation metrics, potentially obfuscating relationships between ω and vegetation.

While the GAM explained nearly three-quarters of the spatial variability in catchment level ω , numerous factors may impede these variables from explaining additional variability. First, uncertainty in predictor

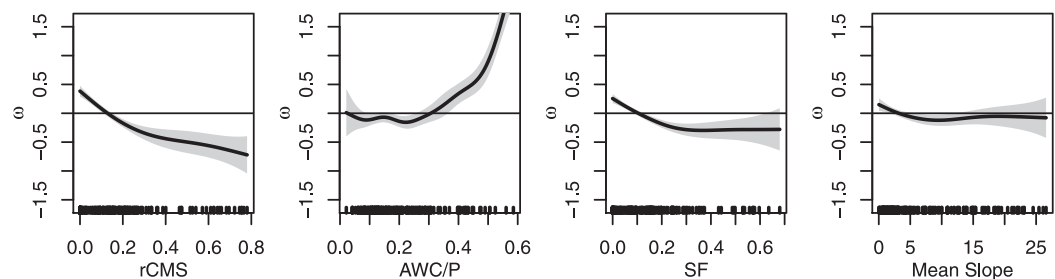


Figure 3. Generalized additive model results explaining ω variability for HCDN watersheds using (from left to right) relative cumulative moisture surplus (rCMS), the ratio of available soil water holding capacity (AWC) to annual precipitation, the fraction of annual precipitation falling as snow (SF), and mean watershed slope. The grey shading in each plot depicts the 95% confidence interval of the relationship, with the black stripes along the x axis denoting the distribution of data from individual watersheds.

variables such as P and ETo estimated from gridded meteorological data sets can be substantial [Newman *et al.*, 2015], particularly in high-elevation watersheds where observations are sparse [e.g., Henn *et al.*, 2015]. Second, the number of ways in which PET can be estimated can lead to discrepancies among studies. Finally, the Budyko equation was designed to capture long-term surface water balance characteristics. This may be problematic in watersheds that have relatively large amounts of interannual variability in Q where monthly climatological estimates (e.g., rCMS) may fail to capture hydroclimate information.

The validation of the ω model with 164 MOPEX watersheds showed good agreement ($r^2 = 0.65$) suggesting the model adequately captured spatial patterns of ω . The slightly lower explained variance in validation may reflect the tendency for MOPEX watersheds to have less stringent requirements of nominal human influence (e.g., irrigation withdrawals, land use changes) than HCDN watersheds. Second, we estimated the mean Q from 1980 to 2010 for MOPEX catchments with equation (1) using observed P and ETo along with modeled ω from the GAM. The Budyko relationship with modeled ω explained 97% of the observed geographic variability in Q with a mean absolute error of 17%. By comparison, using the default ω value of 2.6 explained 94% of the spatial variability in Q with a mean absolute error of 31%.

3.4. Application of Modeled ω to CONUS

The application of the GAM for ω across the CONUS is shown in Figure 4a. A companion set of maps of the predictor variables applied to the GAM are provided in supporting information Figure S1. The mean and median predicted ω over the CONUS was 2.85 and 2.66, respectively, which is close to the default value of 2.6. In contrast to the modest spatial variability in modeled ω for the eastern portion of the CONUS, strong heterogeneity in ω was modeled across much of the western CONUS. Namely, much of the valleys or basins across arid and semiarid portions of the western United States as well as the Great Plains had high ω (>4), coinciding geographically with shallow slopes, high AWC:P ratios, and low rCMS (supporting information

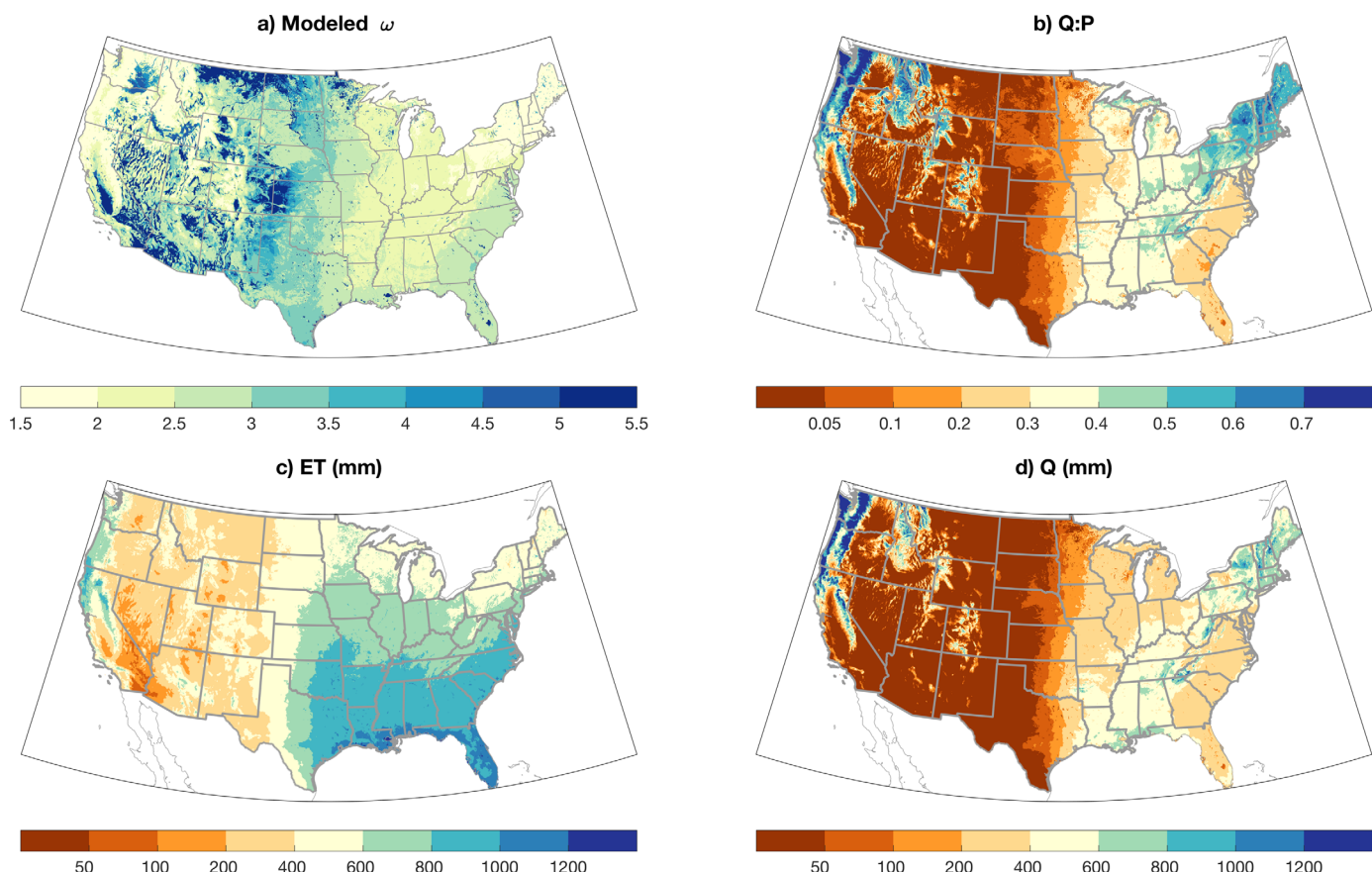


Figure 4. (a) Modeled ω across CONUS derived from the generalized additive model, and estimated (b) ratio of annual streamflow (Q) to annual precipitation (P), (c) evapotranspiration (ET), and (d) Q derived with the Budyko framework for the 1980–2010 period.

Figure S1). By contrast, ω was low (<2) across the mountainous regions of the western US where much of the Q is generated. These regions are typified by shallower soils, greater fraction of annual precipitation falling as snow, higher rCMS, and steeper slopes. As a caveat, since the GAM was clamped by the training data, the ability to extrapolate ω outside of the range of the training watersheds may be limited.

Modeled ω was applied using the Budyko relationship to estimate long-term average ET and Q across the CONUS (Figures 4b–4d). Estimated ET exceeded 800 mm across much of the southeastern US and was less than 400 mm for much of the western United States, whereas Q exceeded 1000 mm for parts of the Cascades, northern Sierra Nevada and coast ranges in California, Oregon, and Washington, with nominal annual Q (<50 mm) across the lower elevations of the western United States. These ET values are similar to other CONUS-scale ET estimates [e.g., Sanford and Selnick, 2013].

We qualitatively compared estimates of ET and ET:P from the Budyko relationship of Fu [1981] to modeled results from the Variable Infiltration Capacity (VIC) model from Livneh *et al.* [2013]. Although comparisons are somewhat flawed due to the use different meteorological forcing data sets, and as the VIC model incorporates sophisticated land-surface algorithms that account for spatial and subgrid heterogeneity in vegetation, topography, and snowpack dynamics, we find substantial commonality between the two results (supporting information Figure S2). Both data sets show similar spatial estimates of ET, with a spatial correlation of 0.92 and mean absolute difference of 69 mm (supporting information Figure S2). Averaged over the CONUS, the fraction of P lost to ET was estimated at 70.1% in the Budyko relationship compared to 69% for VIC.

3.5. Application of Modeled ω to CONUS Climate Change Scenarios

Downscaled climate change projections were input into the ω model to assess the applicability of the ω model under mid-21st century (2040–2069) climate. Whereas changes in the long-term water budget

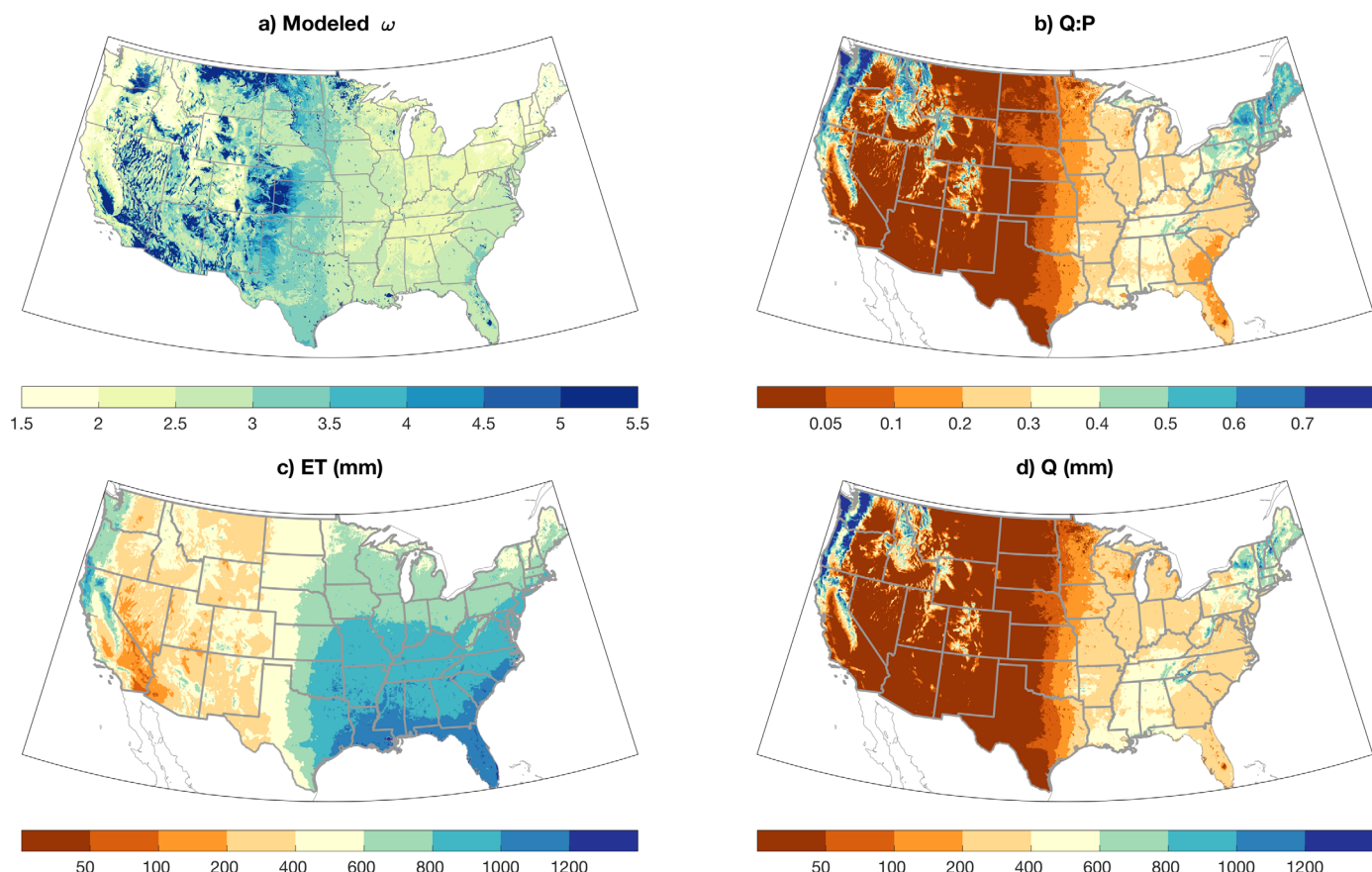


Figure 5. As in Figure 4, but using multimodel mean projected changes in climate for the mid-21st century (2040–2069) under the RCP8.5 forcing experiment.

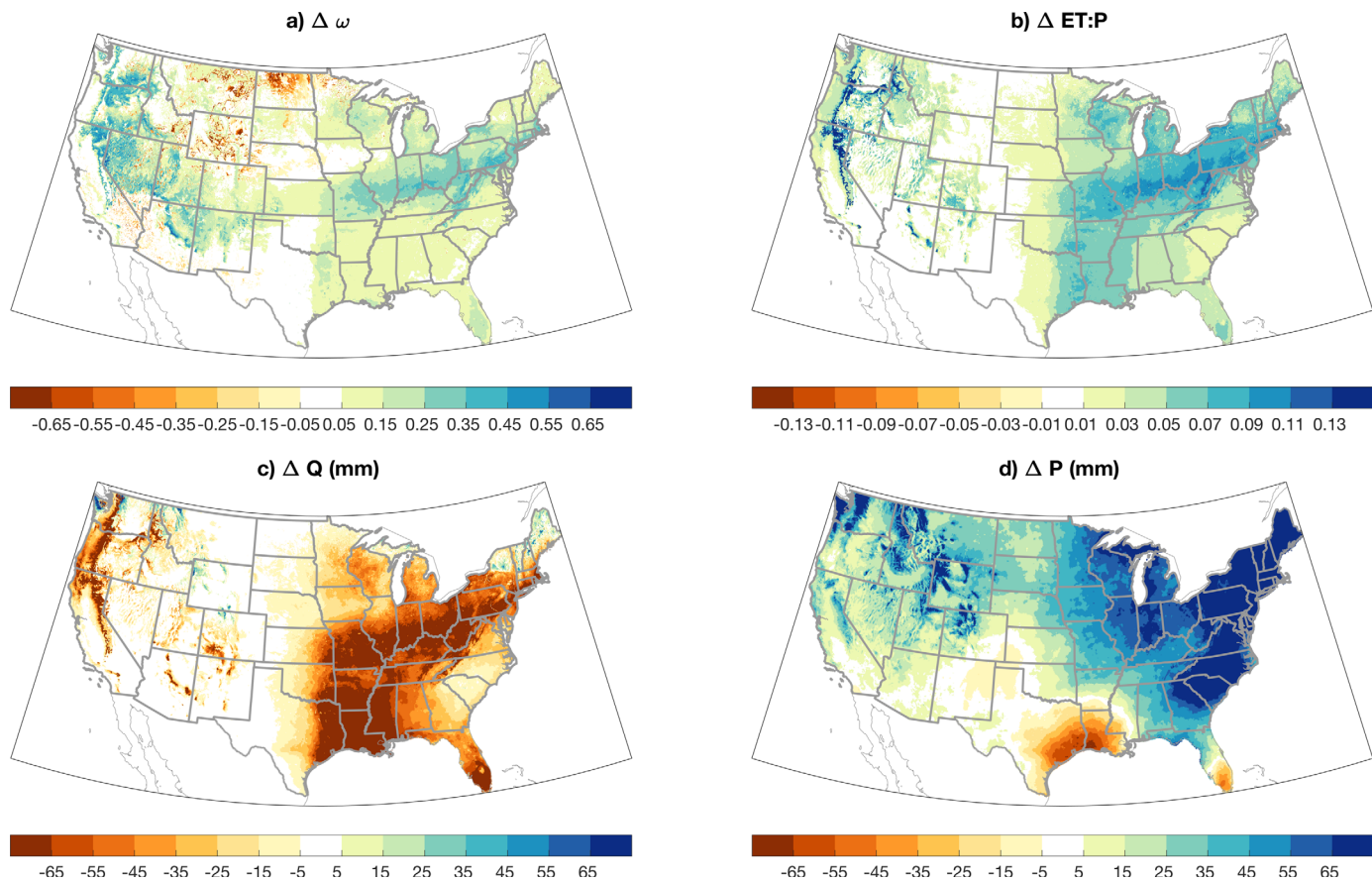


Figure 6. Projected changes expressed as differences between mid-21st century (2040–2069) and the historical period (1980–2010) in (a) ω , (b) the ratio of evapotranspiration to precipitation, (c) runoff (Q), and (d) precipitation.

assessed with the Budyko equation may occur strictly through changing aridity, changes in watershed characteristics that influence precipitation partitioning as in ω may also occur. Modeled ω using the GAM for the mid-21st century exhibited similar spatial patterns to those for the historical period (Figure 5a). However, modeled ω for the mid-21st century showed an average overall increase of about 0.1 for the CONUS, with the largest increase across the mid-to-lower elevations of the intermountain western United States and from Missouri eastward to the Atlantic (Figure 6a). Increased ω , per the GAM, were modeled for regions with reduced SF (particularly where $SF < 0.3$) or declines in rCMS (supporting information Figure S3). Whereas multimodel mean P exhibits nominal change to slight increases across much of the CONUS (Figure 6d), decreased rCMS in a consequence of increased ETo, particularly in regions and months where historical $P - ETo > 0$ and $\Delta ETo > \Delta P$. A few areas of decreased ω were projected across the western United States and northern Plains. These decreases were in arid and semiarid areas where $\Delta P > 0$ and the historical AWC:P > 0.4.

The application of modeled ω and climate projections to the Budyko relationship of Fu [1981] yielded substantial increases in modeled ET across the CONUS (Figure 5c). The model also projects an increase in the fraction of P used by ET (Figure 6b), consistent with both the shift toward larger ω and increases in aridity (supporting information Figure S3) [e.g., Ficklin et al., 2016]. In contrast to increased P across most of the CONUS, the Budyko model projects declines in Q across much of the eastern half of the country, the Colorado River Basin, the Sierra Nevada and the lower elevations of the Cascades (Figure 6c). A few areas of increased Q were modeled across the middle and northern Rockies, the North Cascades, as well as across mountains in the northeastern United States.

Our results largely agree with other studies that used more advanced hydrologic simulations which suggest decreases in surface runoff across the CONUS and increased water scarcity [Milly et al., 2005;

Averyt *et al.*, 2013] under anthropogenic climate change. Note however, that our modeling analysis does not explicitly consider uncertainty in the climate change response across models, but rather just the multimodel mean change in climate. Declines in Q have been modeled under future climatic forcing for most of the CONUS [Hay *et al.*, 2011; Seager *et al.*, 2013; Schewe *et al.*, 2014]. However, some studies show nominal changes in annual Q for portions of the CONUS [e.g., Elsner *et al.*, 2010], while others show increases in Q over much of CONUS potentially due to increases in P and in particular heavy precipitation events [Naz *et al.*, 2016]. Efforts to incorporate measures of precipitation intensity into the Budyko modeling as done in prior studies [e.g., Milly, 1994; Porporato *et al.*, 2004] may help reconcile some of these differences. Finally, we note that differences in climate forcing data including whether data are bias corrected [Ficklin *et al.*, 2016] and how PET is estimated [Donohue *et al.*, 2010; Williamson *et al.*, 2016] confound comparisons across modeling efforts.

4. Conclusions

A model for the ω parameter of Fu [1981] in the Budyko equation was developed for the CONUS. We demonstrated that 81.2% of the spatial variability in ω for HCDN watersheds was explained using four variables (relative cumulative moisture surplus, the ratio of soil water holding capacity to precipitation, topographic slope, and the fraction of precipitation falling as snow) that capture climatic and physiographic facets. Conceptually, our results agree with previous studies that have examined the individual influence of such factors. Moreover, the parameters used to model ω are widely available and therefore the results produced in this work could be expanded to outside of the CONUS.

We did not identify additional value of incorporating vegetation metrics such as NDVI or NPP into the GAM for ω , although variables used in the GAM may explain biogeographic factors that influence vegetation-water dynamics. These results agree with previous research that suggests that climatic characteristics primarily determine precipitation partitioning, with vegetation characteristics playing a lesser role [Sanford and Selnick, 2013]. While climate and physiographic variables are often used to infer potential vegetation distributions, the failure to explicitly account for vegetation dynamics means that the model may be unable to capture water yields in regions with landscape disturbance such as a postfire environment, or in regions that have undergone significant land use change [Hamel and Guswa, 2015]. Likewise, it is unclear whether simple modeled changes in ω capture vegetation dynamics in a changing climate. For example, substantial changes in the partitioning of P to ET may occur in montane watersheds where warming enables an uphill expansion of vegetation [Goulden and Bales, 2014]. Finally, we did not account for the influence of increased CO₂ on water use efficiency thereby potentially over predicting estimates of future PET [Milly and Dunne, 2016]. Likewise, the multiple roles of vegetation dynamics in a changing climate may offset or compound simple modeled estimates [Swann *et al.*, 2016; Ukkola *et al.*, 2016; Mankin *et al.*, 2017]. While these uncertainties undermine the modeled changes in water balance using the Budyko framework, they can also plague other physically based hydrologic models.

The application of the spatial model for ω across the CONUS within the Budyko equation exhibited spatial patterns of the surface water balance that resemble much more model intensive estimates from VIC. While the Budyko framework is simple, it provides an instructive way to rapidly model variability in time-mean catchment water balance to ungauged watershed, and to climate scenarios. However, as such simple modeling efforts effectively rely on space for time substitution, they may be unable to account for nonstationarities in the land-surface water balance that occur in a changing climate [Milly *et al.*, 2008] including methodological choices in estimating PET [Sheffield *et al.*, 2012; Dewes *et al.*, 2017], the influence of increasing CO₂ on PET [Milly and Dunne, 2016], and vegetation dynamics [Swann *et al.*, 2016]. Space-for-time modeling efforts may also be challenged by no-analog climates with a changing climate that may further restrict the geographic extent where models built with contemporary data can be applied. Likewise, the Budyko relationship as applied here only captures the long-term average surface water partitioning it is not able to assess seasonal changes in water balance such as the shift in runoff seasonality with more runoff in winter and early spring at the expense of summer runoff in presently snowmelt-dominated watersheds [Ficklin *et al.*, 2013; Vano *et al.*, 2014]. Despite these shortcomings, the relative ease of applying the Budyko relationship to gauge watershed sensitivity to climate change as well as uncertainty in modeling ω may

help complement other rigorous modeling studies that utilize land-surface hydrology models [e.g., Vano *et al.*, 2014; Clark *et al.*, 2016].

Acknowledgements

We thanks the constructive reviewers from three reviewers who helped improve the clarity of the manuscript. All data sets used in this paper are available from public data repositories. The observed [<http://metdata.northwestknowledge.net/>] and projected [<http://maca.northwestknowledge.net/>] climate data sets used in this work are available through the Northwest Knowledge Network at the University of Idaho. This research was partially supported by the US Department of Agriculture's National Institute of Food and Agriculture grant 2011-68002-30191 and National Science Foundation grant 1639524.

References

- Abatzoglou, J. T. (2013), Development of gridded surface meteorological data for ecological applications and modelling, *Int. J. Climatol.*, 33, 121–131.
- Abatzoglou, J. T., and T. J. Brown (2012), A comparison of statistical downscaling methods suited for wildfire applications, *Int. J. Climatol.*, 32, 772–780.
- Abatzoglou, J. T., R. Barbero, J. W. Wolf, and Z. A. Holden (2014), Tracking interannual streamflow variability with drought indices in the US pacific northwest, *J. Hydrometeorol.*, 15, 1900–1912.
- Allen, R. G., L. S. Pereira, D. Raes, and M. Smith (1998), Crop evapotranspiration-Guidelines for computing crop water requirements-FAO Irrigation and drainage paper 56, FAO Rome, 300, D05109.
- Averyt, K., J. Meldrum, P. Caldwell, G. Sun, S. McNulty, A. Huber-Lee, and N. Madden (2013), Sectoral contributions to surface water stress in the coterminous United States, *Environ. Res. Lett.*, 8, 35046.
- Berghuys, W. R., R. A. Woods, and M. Hrachowitz (2014), A precipitation shift from snow towards rain leads to a decrease in streamflow, *Nat. Clim. Change*, 4, 583–586.
- Bosshard, T., M. Carambia, K. Goergen, S. Kotlarski, P. Krahe, M. Zappa, and C. Schär (2013), Quantifying uncertainty sources in an ensemble of hydrological climate-impact projections, *Water Resour. Res.*, 49, 1523–1536, doi:10.1029/2011WR011533.
- Budyko, M. I. (1974), *Climate and Life*, 508 pp., Academic Press, New York.
- Chebana, F., C. Charron, T. B. M. J. Ouarda, and B. Martel (2014), Regional frequency analysis at ungauged sites with the generalized additive model, *J. Hydrometeorol.*, 15, 2418–2428.
- Clark, M. P., R. L. Wilby, E. D. Gutmann, J. A. Vano, S. Gangopadhyay, A. W. Wood, H. J. Fowler, C. Prudhomme, J. R. Arnold, and L. D. Brekke (2016), Characterizing uncertainty of the hydrologic impacts of climate change, *Curr. Clim. Change Rep.*, 2, 55–64.
- Dai, A. (2008), Temperature and pressure dependence of the rain-snow phase transition over land and ocean, *Geophys. Res. Lett.*, 35, L12802, doi:10.1029/2008GL033295.
- Daly, C., M. Halbleib, J. I. Smith, W. P. Gibson, M. K. Doggett, G. H. Taylor, J. Curtis, and P. P. Pasteris (2008), Physiographically sensitive mapping of climatological temperature and precipitation across the conterminous United States, *Int. J. Climatol.*, 28, 2031–2064.
- Dewes, C. F., I. Rangwala, J. J. Barsugli, M. T. Hobbins, and S. Kumar (2017), Drought risk assessment under climate change is sensitive to methodological choices for the estimation of evaporative demand, *PLoS One*, 12, e0174045.
- Donohue, R. J., M. L. Roderick, and T. R. McVicar (2006), On the importance of including vegetation dynamics in Budyko's hydrological model, *Hydrol. Earth Syst. Sci. Discuss.*, 3, 1517–1551.
- Donohue, R. J., T. R. McVicar, and M. L. Roderick (2010), Assessing the ability of potential evaporation formulations to capture the dynamics in evaporative demand within a changing climate, *J. Hydrol.*, 386, 186–197.
- Donohue, R. J., M. L. Roderick, and T. R. McVicar (2012), Roots, storms and soil pores: Incorporating key ecohydrological processes into Budykos hydrological model, *J. Hydrol.*, 436, 35–50.
- Duan, Q., J. Schaake, V. Andreassian, S. Franks, G. Goteti, H. V. Gupta, Y. M. Gusev, F. Habets, A. Hall, and L. Hay (2006), Model Parameter Estimation Experiment (MOPEX): An overview of science strategy and major results from the second and third workshops, *J. Hydrol.*, 320, 3–17.
- Elsner, M. M., L. Cuo, N. Voisin, J. S. Deems, A. F. Hamlet, J. A. Vano, K. E. B. Mickelson, S.-Y. Lee, and D. P. Lettenmaier (2010), Implications of 21st century climate change for the hydrology of Washington State, *Clim. Change*, 102, 225–260.
- Elsner, M. M., S. Gangopadhyay, T. Pruitt, L. D. Brekke, N. Mizukami, and M. P. Clark (2014), How does the choice of distributed meteorological data affect hydrologic model calibration and streamflow simulations?, *J. Hydrometeorol.*, 15, 1384–1403.
- Ficklin, D. L., I. T. Stewart, and E. P. Maurer (2013), Climate change impacts on streamflow and subbasin-scale hydrology in the Upper Colorado River Basin, *PLoS One*, 8, e71297.
- Ficklin, D. L., J. T. Abatzoglou, S. M. Robeson, and A. Dufficy (2016), The influence of climate model biases on projections of aridity and drought, *J. Clim.*, 29, 1269–1285.
- Fu, B. P. (1981), On the calculation of the evaporation from land surface, *Sci. Atmos. Sin.*, 5, 23–31.
- Gardner, L. R. (2009), Assessing the effect of climate change on mean annual runoff, *J. Hydrol.*, 379, 351–359.
- Gentine, P., P. D'Odorico, B. R. Lintner, G. Sivandran, and G. Salvucci (2012), Interdependence of climate, soil, and vegetation as constrained by the Budyko curve, *Geophys. Res. Lett.*, 39, L19404, doi:10.1029/2012GL053492.
- Goulden, M. L., and R. C. Bales (2014), Mountain runoff vulnerability to increased evapotranspiration with vegetation expansion, *Proc. Natl. Acad. Sci. U. S. A.*, 111, 14,071–14,075.
- Greve, P., L. Gudmundsson, B. Orlofsky, and S. I. Seneviratne (2015), Introducing a probabilistic Budyko framework, *Geophys. Res. Lett.*, 42, 2261–2269, doi:10.1002/2015GL063449.
- Hamel, P., and A. J. Guswa (2015), Uncertainty analysis of a spatially explicit annual water-balance model: Case study of the Cape Fear basin, North Carolina, *Hydrol. Earth Syst. Sci.*, 19, 839–853.
- Hay, L. E., S. L. Markstrom, and C. Ward-Garrison (2011), Watershed-scale response to climate change through the twenty-first century for selected basins across the United States, *Earth Interact.*, 15, 1–37, doi:10.1175/2010EI370.1.
- Henn, B., M. P. Clark, D. Kavetski, and J. D. Lundquist (2015), Estimating mountain basin-mean precipitation from streamflow using Bayesian inference, *Water Resour. Res.*, 51, 8012–8033, doi:10.1002/2014WR016736.
- Jiang, C., L. Xiong, D. Wang, P. Liu, S. Guo, and C.-Y. Xu (2015), Separating the impacts of climate change and human activities on runoff using the Budyko-type equations with time-varying parameters, *J. Hydrol.*, 522, 326–338.
- Krawchuk, M. A. M., M. A. Moritz, M.-A. Parisien, J. Van Dorn, and K. Hayhoe (2009), Global pyrogeography: The current and future distribution of wildfire, *PLoS One*, 4, e5102.
- Li, D., M. Pan, Z. Cong, L. Zhang, and E. Wood (2013), Vegetation control on water and energy balance within the Budyko framework, *Water Resour. Res.*, 49, 969–976, doi:10.1002/wrcr.20107.
- Liang, W., D. Bai, F. Wang, B. Fu, J. Yan, S. Wang, Y. Yang, D. Long, and M. Feng (2015), Quantifying the impacts of climate change and ecological restoration on streamflow changes based on a Budyko hydrological model in China's Loess Plateau, *Water Resour. Res.*, 51, 6500–6519, doi:10.1002/2014WR016589.

- Livneh, B., E. A. Rosenberg, C. Lin, B. Nijssen, V. Mishra, K. M. Andreadis, E. P. Maurer, and D. P. Lettenmaier (2013), A long-term hydrologically based dataset of land surface fluxes and states for the conterminous United States: Update and extensions, *J. Clim.*, **26**, 9384–9392.
- Long, D., L. Longuevergne, and B. R. Scanlon (2014), Uncertainty in evapotranspiration from land surface modeling, remote sensing, and GRACE satellites, *Water Resour. Res.*, **50**, 1131–1151, doi:10.1002/2013WR014581.
- Mankin, J. S., J. E. Smerdon, B. I. Cook, A. P. Williams, and R. Seager (2017), The curious case of projected 21st-century drying but greening in the American West, *J. Clim.*, doi:10.1175/JCLI-D-17-0213.1.
- McCabe, G. J., and D. M. Wolock (2011), Independent effects of temperature and precipitation on modeled runoff in the conterminous United States, *Water Resour. Res.*, **47**, W11522, doi:10.1029/2011WR010630.
- McMahon, T. A., M. C. Peel, G. G. Pegram, and I. N. Smith (2011), A simple methodology for estimating mean and variability of annual runoff and reservoir yield under present and future climates, *J. Hydrometeorol.*, **12**, 135–146.
- Milly, P. C. D. (1994), Climate, soil water storage, and the average annual water balance, *Water Resour. Res.*, **30**, 2143–2156.
- Milly, P. C. D., and K. A. Dunne (2016), Potential evapotranspiration and continental drying, *Nat. Clim. Change*, **6**, 946–949.
- Milly, P. C. D., K. A. Dunne, and A. V. Vecchia (2005) Global pattern of trends in streamflow and water availability in a changing climate, *Nature*, **438**, 347–350.
- Milly, P. C. D., J. Betancourt, M. Falkenmark, R. M. Hirsch, Z. W. Kundzewicz, D. P. Lettenmaier, and R. J. Stouffer (2008), Stationarity is dead: Whither water management?, *Science*, **319** 573–574.
- Mitchell, K. E., et al. (2004), The multi-institution North American Land Data Assimilation System (NLDAS): Utilizing multiple GCIP products and partners in a continental distributed hydrological modeling system, *J. Geophys. Res.*, **109**, D07S90, doi:10.1029/2003JD003823.
- Naz, B. S., S.-C. Kao, M. Ashfaq, D. Rastogi, R. Mei, and L. C. Bowling (2016), Regional hydrologic response to climate change in the conterminous United States using high-resolution hydroclimate simulations, *Global Planet. Change*, **143**, 100–117.
- Newman, A. J., M. P. Clark, J. Craig, B. Nijssen, A. Wood, E. Gutmann, N. Mizukami, L. Brekke, and J. R. Arnold (2015) Gridded ensemble precipitation and temperature estimates for the contiguous United States, *J. Hydrometeorol.*, **16**, 2481–2500.
- Oudin, L., V. Andréassian, J. Lerat, and C. Michel (2008), Has land cover a significant impact on mean annual streamflow? An international assessment using 1508 catchments, *J. Hydrol.*, **357**, 303–316.
- Pausas, J. G., and E. Ribeiro (2013), The global fire-productivity relationship, *Global Ecol. Biogeogr.*, **22**, 728–736.
- Peel, M. C., T. A. McMahon, and B. L. Finlayson (2010), Vegetation impact on mean annual evapotranspiration at a global catchment scale, *Water Resour. Res.*, **46**, W09508, doi:10.1029/2009WR008233.
- Porporato, A., E. Daly, and I. Rodriguez-Iturbe (2004), Soil water balance and ecosystem response to climate change, *Am. Nat.*, **164**, 625–632.
- Potter, N. J., L. Zhang, P. C. D. Milly, T. A. McMahon, and A. J. Jakeman (2005), Effects of rainfall seasonality and soil moisture capacity on mean annual water balance for Australian catchments, *Water Resour. Res.*, **41**, W06007, doi:10.1029/2004WR003697.
- R Core Team (2017), *R Language Definition*; R Found. for Stat. Comput., Vienna, Austria.
- Renard, B., D. Kavetski, G. Kuczera, M. Thyre, and S. W. Franks (2010), Understanding predictive uncertainty in hydrologic modeling: The challenge of identifying input and structural errors, *Water Resour. Res.*, **46**, W05521, doi:10.1029/2009WR008328.
- Roderick, M. L., and G. D. Farquhar (2011), A simple framework for relating variations in runoff to variations in climatic conditions and catchment properties, *Water Resour. Res.*, **47**, W00G07, doi:10.1029/2010WR009826.
- Rodríguez-Iturbe, I., V. Isham, C. R. Cox, S. Manfreda, and A. Porporato (2006), Space-time modeling of soil moisture: Stochastic rainfall forcing with heterogeneous vegetation, *Water Resour. Res.*, **42**, W06D05, doi:10.1029/2005WR004497.
- Running, S. W., R. R. Nemani, F. A. Heinsch, M. Zhao, M. Reeves, and H. Hashimoto (2004), A continuous satellite-derived measure of global terrestrial primary production, *Bioscience*, **54**, 547–560.
- Sanford, W. E., and D. L. Selnick (2013), Estimation of evapotranspiration across the conterminous United States using a regression with climate and land-cover Data1, *J. Am. Water Resour. Assoc.*, **49**, 217–230.
- Sankarasubramanian, A., and R. M. Vogel (2002), Comment on the paper: "Basin hydrologic response relations to distributed physiographic descriptors and climate," *J. Hydrol.*, **263**, 257–261.
- Schaake, J. C., V. I. Koren, Q. Duan, K. Mitchell, and F. Chen (1996), Simple water balance model for estimating runoff at different spatial and temporal scales, *J. Geophys. Res.*, **101**, 7461–7475.
- Schewe, J., J. Heinke, D. Gerten, I. Haddeland, N. W. Arnell, D. B. Clark, R. Dankers, S. Eisner, B. M. Fekete, and F. J. Colón-González (2014), Multimodel assessment of water scarcity under climate change, *Proc. Natl. Acad. Sci. U. S. A.*, **111**, 3245–3250.
- Seager, R., M. Ting, C. Li, N. Naik, B. Cook, J. Nakamura, and H. Liu (2013), Projections of declining surface-water availability for the southwestern United States, *Nat. Clim. Change*, **3**, 482–486.
- Shao, Q., A. Traylen, and L. Zhang (2012), Nonparametric method for estimating the effects of climatic and catchment characteristics on mean annual evapotranspiration, *Water Resour. Res.*, **48**, W03517, doi:10.1029/2010WR009610.
- Sheffield, J., E. F. Wood, and M. L. Roderick (2012), Little change in global drought over the past 60 years, *Nature*, **491**, 435–438.
- Sivapalan, M., K. Takeuchi, S. W. Franks, V. K. Gupta, H. Karambiri, V. Lakshmi, X. Liang, J. J. McDonnell, E. M. Mendiondo, and P. E. O'Connell (2003), IAHS Decade on Predictions in Ungauged Basins (PUB), 2003–2012: Shaping an exciting future for the hydrological sciences, *Hydrolog. Sci. J.*, **48**, 857–880.
- Slack, J. R., J. M. Landwehr, (1992), Hydro-climatic data network (HCDN): A U.S. Geological Survey streamflow data set for the United States for the study of climate variations, 1874–1988, U.S. Geological Survey, Open File Report 92-129, USGS Water Supply Paper No. 2406, 171 pp., Reston, Va.
- Stephenson, N. L. (1990), Climatic control of vegetation distribution: the role of the water balance, *Am. Nat.*, **135**, 649–670.
- Swann, A. L. S., F. M. Hoffman, C. D. Koven, and J. T. Randerson (2016), Plant responses to increasing CO₂ reduce estimates of climate impacts on drought severity, *Proc. Natl. Acad. Sci. U. S. A.*, **113**, 10,019–10,024.
- Ukkola, A. M., T. F. Keenan, D. I. Kelley, and I. C. Prentice (2016), Vegetation plays an important role in mediating future water resources, *Environ. Res. Lett.*, **11**, 94022.
- Vano, J. A., and D. P. Lettenmaier (2014), A sensitivity-based approach to evaluating future changes in Colorado River discharge, *Clim. Change*, **122**, 621–634.
- Vano, J. A., B. Udall, D. R. Cayan, J. T. Overpeck, L. D. Brekke, T. Das, H. C. Hartmann, H. G. Hidalgo, M. Hoerling and G. J. McCabe (2014), Understanding uncertainties in future Colorado River streamflow, *Bull. Am. Meteorol. Soc.*, **95**, 59–78.
- Vörösmarty, C. J., P. Green, J. Salisbury, and L. B. Lammers (2000), Global water resources: Vulnerability from climate change and population growth, *Science*, **289**, 284–288.
- Wang, C., S. Wang, B. Fu, and L. Zhang (2016), Advances in hydrological modelling with the Budyko framework A review, *Prog. Phys. Geogr.*, **40**, 409–430.

- Wilby, R. L., and I. Harris (2006), A framework for assessing uncertainties in climate change impacts: Low-flow scenarios for the River Thames, UK, *Water Resour. Res.*, **42**, W02419, doi:10.1029/2005WR004065.
- Williamson, T. N., E. A. Nystrom, and P. C. D. Milly (2016), Sensitivity of the projected hydroclimatic environment of the Delaware River basin to formulation of potential evapotranspiration, *Clim. Change*, **139**, 215–228.
- Wolock, D. M., and G. J. McCabe (1999), Explaining spatial variability in mean annual runoff in the conterminous United States, *Clim. Res.*, **11**, 149–159.
- Wood, S., and M. S. Wood (2017), *Package ‘mgcv’*. R package version 1–7.
- Xu, X., W. Liu, B. R. Scanlon, L. Zhang, and M. Pan (2013), Local and global factors controlling water-energy balances within the Budyko framework, *Geophys. Res. Lett.*, **40**, 6123–6129, doi:10.1002/2013GL058324.
- Xu, X., D. Yang, H. Yang, and H. Lei (2014), Attribution analysis based on the Budyko hypothesis for detecting the dominant cause of runoff decline in Haihe basin, *J. Hydrol.*, **510**, 530–540.
- Yang, D., F. Sun, Z. Liu, Z. Cong, G. Ni, and Z. Lei (2007), Analyzing spatial and temporal variability of annual water-energy balance in non-humid regions of China using the Budyko hypothesis, *Water Resour. Res.*, **43**, W04426, doi:10.1029/2006WR005224.
- Zhan, C. S., C. W. Niu, S. M. Song, and C. Y. Xu (2013), The impacts of climate variability and human activities on streamflow in Bai River basin, northern China, *Hydrol. Res.*, **44**, 875–885.
- Zhang, L., W. R. Dawes, and G. R. Walker (2001), Response of mean annual evapotranspiration to vegetation changes at catchment scale, *Water Resour. Res.*, **37**, 701–708.
- Zhang, L., K. Hickel, W. R. Dawes, F. H. S. Chiew, A. W. Western, and P. R. Briggs (2004), A rational function approach for estimating mean annual evapotranspiration, *Water Resour. Res.*, **40**, W02502, doi:10.1029/2003WR002710.
- Zhang, S., H. Yang, D. Yang, and A. W. Jayawardena (2016), Quantifying the effect of vegetation change on the regional water balance within the Budyko framework, *Geophys. Res. Lett.*, **43**, 1140–1148, doi:10.1002/2015GL066952.
- Zhou, G., X. Wei, X. Chen, P. Zhou, X. Liu, Y. Xiao, G. Sun, D. F. Scott, S. Zhou, L. Han, and Y. Su (2015), Global pattern for the effect of climate and land cover on water yield, *Nat. Commun.*, **6**, 5918.